Journal of Catalysis 295 (2012) 254–260

Contents lists available at SciVerse ScienceDirect

Journal of Catalysis

journal homepage: www.elsevier.com/locate/jcat

Visible-light-induced oxidation of *trans*-ferulic acid by TiO_2 photocatalysis

F. Parrino [a], V. Augugliaro [a], G. Camera-Roda [b], V. Loddo [a], M.J. López-Muñoz [c], C. Márquez-Álvarez [d], G. Palmisano [a], L. Palmisano [a,*], M.A. Puma [a]

[a] "Schiavello-Grillone" Photocatalysis Group, Dipartimento di Ingegneria Elettrica Elettronica e delle Telecomunicazioni, di tecnologie Chimiche, Automatica e modelli Matematici (DIEETCAM), University of Palermo, Viale delle Scienze, Ed. 6, 90128 Palermo, Italy
[b] Dipartimento di Ingegneria Chimica, University of Bologna, Via Terracini 28, 40131 Bologna, Italy
[c] Department of Chemical and Environmental Technology, ESCET, Rey Juan Carlos University, C/Tulipán s/n, 28933 Móstoles, Madrid, Spain
[d] Instituto de Catálisis y Petroleoquímica, CSIC, C/Marie Curie 2, 28049 Cantoblanco, Madrid, Spain

ARTICLE INFO

Article history:
Received 17 July 2012
Revised 20 August 2012
Accepted 21 August 2012
Available online 25 September 2012

Keywords:
trans-Ferulic acid photo-oxidation
Visible-light photocatalysis
TiO_2
Charge-transfer complex

ABSTRACT

The oxidation of *trans*-ferulic acid ($C_{10}H_{10}O_4$) in aqueous TiO_2 dispersion occurs via the formation of a charge-transfer complex on the TiO_2 surface that is able to absorb visible light ($\lambda \geqslant 400$ nm). The main product is CO_2, whereas secondary oxidation products are organic species such as vanillin, caffeic acid, homovanillic acid, and vanillylmandelic acid. Oxidation through the formation of a charge-transfer complex occurs only in the presence of specific TiO_2 samples. Experiments in the absence of oxygen, in the presence of bromate ions and by using a phosphate-modified TiO_2, have been carried out for investigating the reaction mechanism. In order to study the interaction between *trans*-ferulic acid and TiO_2 surface and to characterize the charge-transfer complex, UV–Vis diffuse reflectance and FT-IR spectroscopies have been used. FT-IR characterization of TiO_2 samples in contact with the aqueous *trans*-ferulic acid solution indicates that the charge-transfer complex formation occurs via adsorption of bidentate ferulate species.

1. Introduction

Among the advanced oxidation processes, photocatalysis in the presence of an irradiated semiconductor has proven to be very effective in the field of environmental remediation [1–6]. Despite the great research activity in the last two decades for obtaining a photocatalyst with optimal features, TiO_2 remains a benchmark against which any alternative photocatalyst must be compared. TiO_2 is indeed one of the most attractive photocatalytic materials due to its low cost, good chemical and photochemical stability, and nontoxicity. In general, pure TiO_2 with its large band gap (3.2 eV for anatase) can be activated only by near-UV light ($\lambda < 385$ nm), which represents a small fraction of solar light (about 3–4%). This inactivity under visible light strongly limits the practical application of TiO_2 photocatalyst. In order to overcome this drawback, pure TiO_2 has been modified by impurity doping and dye sensitization.

The doping has been done with ions of transitional metals, such as Co, Cr, Cu, Fe, Mn, Ni and V [7–10], and also of nonmetals such as B, C, N and S [11–14]. Recently, new visible responsive photocatalysts were prepared by modification of TiO_2 surface with noble metal complexes or nanoparticles. In particular, Au nanoparticles supported on TiO_2 have been successfully used for the oxidation of alcohols and for the reduction of nitrobenzene under visible irradiation [15]. The main drawback of these methods, however, is that the doping sites could act as recombination centers for the photoexcited electron–hole pairs. Consequently, sometimes the activity of these TiO_2-based photocatalysts does not improve.

In the dye sensitization, organic molecules coated on the TiO_2 surface are used to harvest incident light. Light absorption by the dye is followed by an electron injection from the excited state of the dye molecule into the conduction band of the semiconductor. The remaining positive hole is scavenged by a redox couple on the TiO_2 surface [16]. In the majority of dye-sensitized photoreactions, the dye molecule does not change its chemical nature in the course of the whole process. Another mechanism, called surface-complex charge-transfer mechanism, can be effective for the utilization of visible light. Dimitrijevic et al. [17] showed that the modification of TiO_2 nanoparticles with dopamine enables harvesting of visible light and promotes spatial separation of charges. Fullerol-modified TiO_2 exhibits visible-light photocatalytic activity [18]; in this case, the sensitization works through a single-step process, in which an electron is injected from a surface fullerol–TiO_2 complex to TiO_2 without involving the excited state of fullerol. This system is able to drive both photooxidative and photoreductive conversions, including the redox conversion of 4-chlorophenol, I^-, and Cr(VI) and also the H_2 production. The degradation of salicylic acid under visible light [19] is ascribed to the formation of surface complexes of H_2O_2/TiO_2; the proposed reaction mechanism involves a photoinduced electron transfer of the surface complexes Ti–OOH. A complex between the TiO_2 surface and the

* Corresponding author.
E-mail address: leonardo.palmisano@unipa.it (L. Palmisano).

0021-9517/$ - see front matter © 2012 Elsevier Inc. All rights reserved.
http://dx.doi.org/10.1016/j.jcat.2012.08.018

nonionic surfactant having polyoxyethylene groups (Brij) exhibits visible-light activity for the reduction of CCl_4 and Cr(VI) [20]; the Brij/TiO_2 complex shows a broad absorption band in the 320–500 nm range. In the radical chain reaction of photosulfoxidation of alkanes, the starter radical is generated through absorption of visible light by the TiO_2–SO_2 complex [21]. Kim and Choi [22] investigated on the formation of surface complex between TiO_2 and EDTA, a common electron donor. The complex can absorb visible light through ligand-to-metal charge-transfer (LMCT) mechanism, and its activity is outstanding among all tested TiO_2–substrate complexes, giving rise to the photoreduction of Cr(VI) and production of H_2.

In some cases of dye-sensitized photoreactions, however, the same dye molecules change their chemical nature in the course of the whole process. Trichlorophenol in water forms a charge-transfer complex with TiO_2 that is activated by light wavelengths as long as 520 nm [23]. The trichlorophenoxyl radicals, resulting from charge-transfer, couple with each other to form a set of poly-aromatic chlorinated products, whose distribution is also affected by the light energy [24]. The degradation reaction of phenol, 2,4-dichlorophenol, and 4-chlorophenol in aqueous suspension of pure TiO_2 occurs under visible illumination ($\lambda > 420$ nm) by generating chlorides and CO_2 [25]. The surface complexation between phenolic compounds and TiO_2 appears to be responsible for the reactivity. The selective oxidation of benzyl alcohol to benzaldehyde under visible light in acetonitrile [26] proceeds through the formation of a characteristic complex of a benzyl alcoholic compound on the TiO_2 surface. The surface complexation mechanism is operative in the degradation of RS-2-(4-chloro-o-tolyloxy)propionic acid (mecoprop) on TiO_2 under visible light [27]. TiO_2 treated with mecoprop absorbs also in the visible region; the corresponding FTIR investigation showed that a charge-transfer complex between TiO_2 and mecoprop is formed through carboxylate formation.

This paper reports the results of a study in which *trans*-ferulic acid (FA, $C_{10}H_{10}O_4$, Fig. 1) is oxidized in aqueous TiO_2 dispersion irradiated by visible light. The oxidation process occurs through the formation of a charge-transfer complex able to absorb visible light ($\lambda \geqslant 400$ nm); it must be outlined that FA not only forms a complex on TiO_2 surface, but also itself undergoes the oxidation reactions. The photocatalytic oxidation of FA has been recently investigated under near-UV irradiation as a method both for water detoxification [28] and for chemical production of vanillin [29].

In this study, different commercial and home-prepared TiO_2 samples have been tested and a tentative mechanism to explain the occurrence of the photo-oxidation of FA up to CO_2 has been hypothesized. The interactions between FA and TiO_2 surface have been studied by means of UV–Vis diffuse reflectance and FT-IR spectroscopies.

2. Experimental

The photoreactivity experiments were performed by using two commercial TiO_2 samples, that is, Degussa P25 (ca. 80% anatase and 20% rutile, BET specific surface area, SSA, 50 $m^2 g^{-1}$) and Merck (100% anatase, SSA: 10 $m^2 g^{-1}$), and three home-prepared anatase TiO_2 samples (hereafter denoted as HPC3, HP1/50, and HP0.5). A P25 TiO_2 sample was modified by surface impregnation with phosphate ions. Also Al_2O_3 (Fluka type 507 C neutral, for chromatography) and SiO_2 (silica gel for column chromatography, Riedel-de Haën) were used for blank experiments.

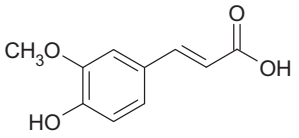

Fig. 1. Chemical structure of ferulic acid.

The amount of catalyst used for the runs was 0.6 g L^{-1} for HPC3, HP1/50, and HP0.5, while it was 0.8 g L^{-1} for Merck and 1 g L^{-1} for the other powders. A systematic study on the dependence of the reactivity on the catalyst amount was performed only in the case of P25 TiO_2.

All the preparation details of HPC3, HP1/50, and HP0.5 samples are reported elsewhere [30–32]. In the following, only some essential information is reported. The HPC3 sample was prepared through a sol–gel route ex $TiCl_4$ (purity > 97%, Fluka) whose hydrolysis in water ($TiCl_4$/water = 1:11 v:v) produced a white sol that upon stirring for 10 h became a clear solution. Then, the suspension was dried and the sol was heated at 673 K for 3 h producing a powder with SSA of 35 $m^2 g^{-1}$. For HP1/50 sample, the precursor solution was obtained by adding 20 mL of $TiCl_4$ to 1000 mL water contained in a volumetric flask; the addition was carried out very slowly without agitation in order to avoid the overheating of solution as the $TiCl_4$ hydrolysis is highly exothermic. At the end of the addition, the resulting solution was mixed for 2 min by a magnetic stirrer and then the flask was sealed and maintained at room temperature (ca. 298 K) for a total aging time ranging from 4 to 9 days. The sol became a transparent solution after ca. 12 h aging, and then, after waiting a few days, the precipitation process started. The colloidal dispersion was then dialyzed by using a dialysis tubing cellulose membrane (average flat width: 76 mm, Sigma Aldrich) until only a negligible amount of chloride ions was detected. The solid was then separated by centrifugation (20 min at 5000 rpm) and dried at room temperature by obtaining a powder with SSA of 118 $m^2 g^{-1}$. For the HP0.5 sample, the precursor solution was obtained by slowly adding 5 mL of $TiCl_4$ drop wise into 50 mL of water in a beaker under magnetic stirring. After that, the beaker was closed and mixing was prolonged for 12 h at room temperature, eventually obtaining a clear solution. This solution was boiled at 373 K for 0.5 h obtaining a white suspension that was then dried at 323 K in order to obtain the final solid consisting mainly of amorphous TiO_2 and crystals of anatase (75%) and rutile (25%). The powder was finally washed with distilled water and centrifuged several times until the chloride ion concentration in the washing water reached a negligible value.

Modification of P25 TiO_2 with phosphate was carried out as follows: 1 g of P25 TiO_2 and 2.76 g of NaH_2PO_4 (Sigma–Aldrich, >98% assay) were suspended in 50 mL water and mixed for 12 h. Then, the powder was recovered by centrifugation and suspended again in 50 mL of fresh NaH_2PO_4 solution. This operation was repeated two more times and then the powder was dried under vacuum at room temperature and finally ground.

Photocatalytic runs were performed by using a cylindrical batch photoreactor (CPR, internal diameter: 32 mm; height: 188 mm) of Pyrex glass. The photoreactor was provided with ports in its upper section for the inlet and outlet of gases and for sampling. A 100 W 12 V halogen display/optic lamp (Osram GmbH, Germany) was axially positioned within the photoreactor. In order to cool the lamp and to cut off light emitted at $\lambda < 400$ nm (which was actually present in very small amount in the emission spectrum of the lamp), a 1 M aqueous solution of $NaNO_2$ (Sigma–Aldrich, >98% assay) was recirculated by means of a peristaltic pump through the Pyrex thimble surrounding the lamp. The radiation energy impinging on the suspension had an average value of 0.4 W cm^{-2}; it was measured between 450 and 950 nm by using a Delta Ohm 9721 radiometer. The aqueous suspension of TiO_2 (temperature of ca. 300 K; volume of 150 mL; catalyst amount: 0.6–3.0 g L^{-1}) was magnetically stirred, and air at atmospheric pressure was bubbled for 0.5 h before starting the runs and during the runs; the initial FA concentration was always 0.5 mM and initial pH ranged between 3.2 and 3.9. For a few runs, pure nitrogen was bubbled into the

suspension and bromate ion (e.g. $KBrO_3$, Sigma–Aldrich, >98%) was added to act as electron trap. During the photoreactivity runs, samples for analyses were withdrawn at fixed times; they were immediately filtered through 0.25 or 0.45 μm membranes (HA, Millipore) to separate catalyst particles.

Measurements of FA adsorption onto the catalysts in the dark were performed by suspending 1.11 g L^{-1} of the catalysts in solutions with different substrate concentrations. After 5 h stirring, the equilibrium was safely reached and the concentration of FA was measured.

The quantitative determination and identification of FA and its oxidation products were performed by means of a Beckman Coulter HPLC (System Gold 126 Solvent Module and 168 Diode Array Detector), equipped with a Phenomenex Synergi 4 μm Hydro-RP 80A column at 298 K. The eluent consisted of a mixture of methanol and 1 mM trifluoroacetic acid aqueous solution (55:45 v:v); its flow rate was 0.6 mL min^{-1}. A UV detector measured the absorbance at 260 nm. Species were identified by comparing their retention times and UV–Vis spectra with those of standards. In order to determine the concentration of bromide and bromate ions, ion chromatography (IC) analyses were carried out by a Dionex DX 120 instrument equipped with an IonPacAS14A column (4 × 250 mm). The eluent was an 8.0 mM Na_2CO_3/1.0 mM $NaHCO_3$ buffer solution. Mineralization extent was evaluated by total organic carbon (TOC) determination carried out by a 5000 A Shimadzu analyzer.

Standards of FA, vanillylmandelic acid, homovanillic acid, vanillin, caffeic acid, 3-methoxycinnamic acid, $KBrO_3$, KBr, and NaH_2PO_4 were purchased from Sigma–Aldrich and used as received. All the other used compounds were reagent grade.

In order to investigate the electronic properties of the charge-transfer complex produced by the interaction between FA and the TiO_2 surface, 50 mg of the catalysts was suspended in 50 mL of 0.5 mM FA aqueous solution for 1 h; then, the suspension was dried under vacuum at 323 K and the resulting sample, spread onto $BaSO_4$ plates, was characterized by diffuse reflectance spectra recorded on a Shimadzu UV-2401PC UV–Vis spectrophotometer. Reflectance data were converted by the instrument software to $F(R_\infty)$ values proportional to absorbance according to the Kubelka–Munk theory [33].

The adsorption in the dark of FA on TiO_2 catalysts was studied by attenuated total reflection-Fourier transform infrared (ATR-FTIR) spectroscopy. ATR-FTIR spectra were recorded using a Thermo Nicolet Nexus 670 FTIR spectrometer equipped with a liquid nitrogen-cooled MCT detector. A SensIR Technologies DurasamplIR horizontal ATR accessory with a stainless steel trough plate was used. The internal reflection element was a diamond-faced ZnSe prism, the incidence angle was 45° and total number of reflections was 9. The trough above the ATR crystal was ca. 4 mm in diameter and had an approximate capacity of 50 μL. Thin films of TiO_2 particles were deposited by placing 20 μL of suspension (2.5 g L^{-1} in Milli-Q deionized water) on the surface of the ATR crystal and evaporating to dryness at room temperature under vacuum. The procedure was repeated four times to obtain thin films containing ca. 200 μg TiO_2. Adsorption of FA was carried out at room temperature by depositing a stock aqueous solution (40 μL, 0.5 mM) on the coated crystal. Infrared spectra were recorded while keeping the sample in the dark for 2 h. Each spectrum was obtained as the average of 1000 scans, with 4 cm^{-1} resolution. Spectra were ratioed against a background spectrum recorded after depositing 20 μL Milli-Q deionized water on the TiO_2-coated crystal. This procedure allowed to eliminate from the spectra absorption bands due to water and titania and thus to reveal only bands corresponding to organic species both adsorbed and in solution. In order to evaluate the contribution of species present in the solution phase, the spectrum of the 0.5 mM FA aqueous solution deposited on the bare ATR crystal was recorded and ratioed against a background spectrum corresponding to deionized water deposited on the bare crystal. For reference purposes, the spectrum of FA dissolved in chloroform (Panreac, 99.0% trichloromethane stabilized with ethanol) was also recorded using the bare ATR plate. Contribution of bands due to chloroform was removed by relating this spectrum against the spectrum of chloroform.

Simultaneous thermal gravimetric (TG/DTG) and differential thermal analysis (DTA) measurements were performed on catalysts by using a Perkin Elmer STA 6000 system, in the 30–750 °C range under a nitrogen flux of ca. 20 mL min^{-1}. The temperature program consisted of three steps: temperature scan from 30 to 120 °C at 10 °C min^{-1}, 15 min in isothermal condition at 120 °C, and temperature scan from 120 to 750 at 10 °C min^{-1}.

3. Results and discussion

Table 1 reports BET specific surface areas and the degree of surface hydroxylation of catalysts, along with their photoactivity performances expressed by the percentage values of FA conversion and mineralization after 180 min of visible irradiation.

According to literature [34], the weight losses of hydroxylated TiO_2 samples in the range 120–600 °C can be related to weakly bonded and strongly bonded OH groups. In Table 1, the global weight losses of OH groups are reported. It can be seen that the home-prepared samples are the most hydroxylated ones with values of 10.75% w/w for HP0.5, 4.66% w/w for HP1/50, and 1.81% w/w for HPC3. The commercial samples showed values of 0.78% w/w for P25 TiO_2 and 0.11% w/w for Merck TiO_2.

The results of adsorption experiments have been modelled by applying the Langmuir model linearized in the following way:

$$\frac{1}{N} = \frac{1}{N_0 K C_L} + \frac{1}{N_0} \quad (1)$$

where N are the adsorbed moles, N_0 the monolayer adsorbed moles, and K the adsorption equilibrium constant. Fig. 2 shows that the Langmuir isotherm fits satisfactorily the experimental adsorption data obtained with HP0.5, HPC3, HP1/50, and P25 TiO_2 samples. SiO_2 and Al_2O_3 also adsorbed the substrate while TiO_2 Merck, surprisingly, did not adsorb. The K values were found equal to 6207.98, 7709.38, 12903.47, and 12346.32 M^{-1} for HP0.5, HP1/50, HPC3, and P25 TiO_2, respectively. The maximum amount of FA that could be adsorbed per gram of catalyst, N_0, was found to be equal to 0.55, 0.21, 0.10, and 0.08 mmol g^{-1} for HP0.5, HP1/50, HPC3, and P25 TiO_2, respectively. A qualitative effect of temperature was also studied and, notably, the amount of adsorbed substrate increased by increasing the suspension temperature from room temperature to 323 K. The latter behavior can be ascribed to the occurrence of chemisorption rather than physisorption, as the predominant phenomenon.

One can observe that the higher the amount of surface hydroxylation of the catalyst, the higher FA adsorption. On the other hand,

Table 1
BET specific surface areas (SSA), % w/w of global surface OH groups, conversion (X) and mineralization after 180 min irradiation.

Powder	SSA (m^2 g^{-1})	OH tot. (% w/w)	X (%)	Mineralization (%)
P25 TiO_2	50	0.78	70	18
Merck TiO_2	10	0.11	0.0	0.0
HP1/50	118	4.66	80	72
HPC3	35	1.81	84	66
HP0.5	235	10.75	100	89
SiO_2	–	–	0.0	0.0
Al_2O_3	–	–	0.0	0.0

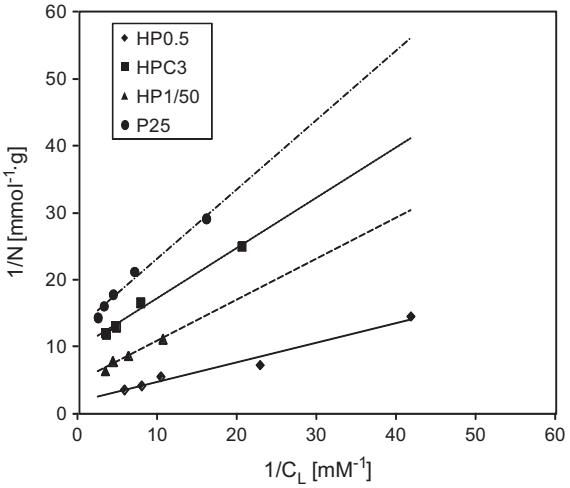

Fig. 2. Adsorption isotherms of FA on HP0.5, HPC3, HP1/50, and P25 TiO_2. Plots represent Langmuir theoretical model, whereas symbols stand for experimental values.

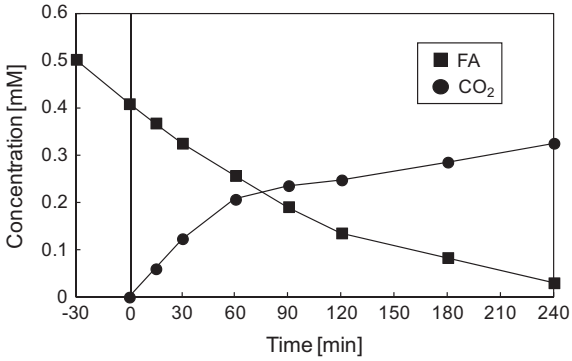

Fig. 3. Concentration of *trans*-ferulic acid (FA) and of normalized carbon dioxide (i.e., divided by 10) versus irradiation time in the presence of air for a representative run. Photocatalyst: HP1/50 (0.6 g L^{-1}). Ignition of the lamp at time = 0.

photocatalytic mineralization (reported in Table 1) notably follows the trends of FA adsorption (Fig. 2), thus showing that the higher the amount of the adsorbed substrate, the higher the mineralization is. A similar trend may be also observed for conversion data.

The oxidation of FA in aqueous medium under visible-light irradiation occurred only in the presence of home-prepared TiO_2 samples and P25 TiO_2; Merck TiO_2, SiO_2, and Al_2O_3 samples were inactive. All the active powders, when suspended in FA solution, turned their color from white to different yellow nuances depending on the catalyst. These suspensions were stable under dark conditions. Irradiation by visible light of suspensions of yellow-colored P25 TiO_2, HP0.5, HP1/50, and HPC3 samples produced the complete mineralization of FA after a maximum time of 10 h, eventually decoloring the catalyst surface. The main oxidation product was CO_2. Vanillin was the most abundant intermediate product detected by means of HPLC; other detected aromatic intermediates were caffeic acid, obtained from FA by substitution of a methoxy group with an –OH one, homovanillic acid and vanillylmandelic acid, both intermediates of vanillin production, and vanillic acid, which derives from vanillin overoxidation. Among open-ring species, only oxalic, formic, and acetic acids were identified by means of ion chromatography. It is worth noting that the products deriving from FA oxidation with the same catalysts but under near-UV irradiation [29], identified by HPLC chromatography too, were almost the same as in the case of visible irradiation.

For a representative run, Fig. 3 shows the concentration of FA and CO_2 versus irradiation time. Notably, after starting visible irradiation of the suspensions, no photo-isomerization of FA was noticed, whereas in the case of near-UV irradiation, *trans*-ferulic acid partially transformed in *cis*-ferulic acid after few minutes [29]. Fig. 3 shows that FA almost completely reacted after 4 h visible irradiation. The concentration of produced CO_2 has been calculated by the measurement of the total organic carbon amount. It can be observed that the production of CO_2 starts with the ignition of the lamp. This behavior indicates that a part of the TiO_2 surface is able to directly perform the mineralization of the organic substrate through the consecutive oxidation of adsorbed intermediate species, which do not desorb from the surface [35]. The data of Fig. 3 also show that FA desorption or adsorption phenomena do not occur after switching on the lamp, thus indicating that the catalyst is not able to be excited by the visible light and therefore to give rise to photoadsorption or photodesorption.

P25 TiO_2 and home-prepared catalysts (HP1/50, HPC3, and HP0.5) gave rise to conversions in the 70–100% range, whereas no reaction occurred in the presence of Merck TiO_2, SiO_2, and Al_2O_3. The vanillin concentration reached a maximum of ca. 0.01 mM in the first hours and remained virtually constant during the course of reaction. The concentrations of homovanillic acid, vanillylmandelic acid, and vanillic acid varied between 0.5 and 5 μM for runs carried out using the different catalysts. Formic acid reached a concentration between 7 and 10 μM for runs carried out with HP1/50, HP0.5, and HPC3, whereas its concentration reached a value of 2 μM by using P25 TiO_2. Acetic acid maximum concentration was 20 μM in runs carried out by using HP1/50 and HPC3, whereas the concentration reached in the presence of HP0.5 and P25 TiO_2 was about 1 μM. The concentrations of oxalic acid ranged between 0.2 and 2 μM for all the used catalysts.

By considering that bare TiO_2 is unable to absorb visible light and FA does not react in the absence of TiO_2 (neither in homogeneous system nor in the presence of SiO_2 and Al_2O_3), the experimental findings that (i) active samples change their color in the presence of FA; (ii) the mineralization percentage increases by increasing the amount of adsorbed FA; and (iii) photo-oxidation of FA occurs under visible-light irradiation ($\lambda \geqslant 400$ nm) may be explained by hypothesizing the formation of a charge-transfer complex between TiO_2 and FA. In order to verify the presence of a light absorbing species on the TiO_2 surface, diffuse reflectance spectra were recorded. In Fig. 4A, the absorbance spectra of pure FA and bare TiO_2 HP1/50 are compared with that of the same TiO_2 after wet impregnation with FA solution (spectrum HP1/50&FA). The spectrum reported in Fig. 4B is obtained by difference between the spectrum HP1/50&FA and that obtained by the sum of HP1/50 and FA spectra.

Comparison of the reflectance spectra in Fig. 4A clearly indicates broad visible absorption between 400 and 600 nm with a maximum between 400 and 420 nm (see Fig. 4B). The other home-prepared catalysts and P25 TiO_2 showed similar behavior. It is worth noting that this absorption widely matches with the solar emission spectrum, although the latter presents a maximum at ca. 600 nm.

The diffuse reflectance spectra obtained indeed by using TiO_2 Merck (Fig. 4C and D), SiO_2, and Al_2O_3 (spectra not reported) showed similar features. For Merck TiO_2, it can be noticed that no novel absorption, coming from the difference between the spectrum Merck&FA and the sum of Merck and FA, is present. Thus, TiO_2 Merck, as also SiO_2 and Al_2O_3 samples, did not give rise to charge-transfer complex formation with a new band absorption and notably they did not show any photocatalytic activity under visible-light irradiation.

Merck TiO_2 was active under near-UV irradiation, but in this condition, it works according to the well-known redox mechanism involving the photoexcitation of the solid [29]. Despite a strong

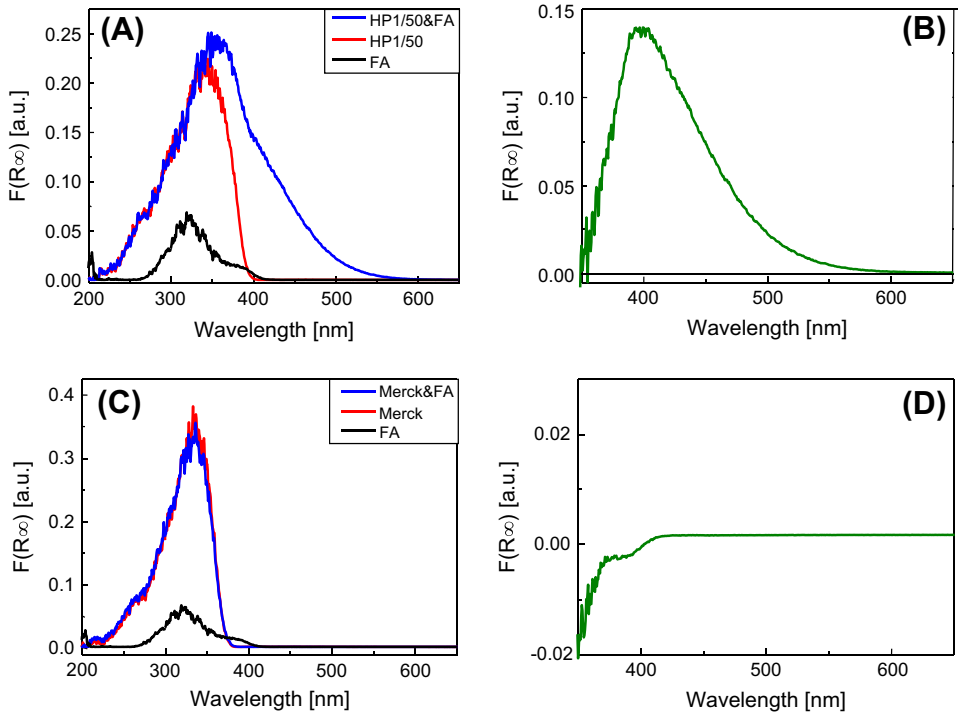

Fig. 4. (A) Reflectance spectra of pure FA (black), pure HP1/50 (red), and HP1/50 upon wet impregnation with FA solution (blue); (B) Spectrum obtained by [HP1/50&FA – (HP1/50 + FA)]; (C) Reflectance spectra of pure FA (black), pure Merck TiO_2 (red) and Merck TiO_2 upon wet impregnation with FA solution (blue); (D) Spectrum obtained by [Merck&FA – (Merck + FA)]. (For interpretation of the references to color in this figure legend, the reader is referred to the web version of this article.)

adsorption of FA onto SiO_2 and Al_2O_3 samples, no change in the reflectance spectra of the powders as well as no color modification were noticed, then evidencing the absence of complex formation. Indeed, SiO_2 and Al_2O_3 do not have a low lying conduction band, differently from TiO_2, compatible with electron transfer from FA to TiO_2.

Interaction between FA and TiO_2 surface was studied by means of an FTIR investigation. ATR-FTIR spectra of the photocatalysts in contact with an aqueous solution of FA at room temperature and in the dark were recorded at given time intervals for a 2-h period. A fast initial development of absorption bands was observed for P25 TiO_2 as well as for home-prepared samples. Bands' growth decayed quickly after several minutes, and a nearly constant intensity was reached after 2 h, while the relative intensity of bands was maintained. Fig. 5 shows ATR-FTIR spectra of these samples in contact with the FA aqueous solution for 2 h (spectra a–d). A contribution of FA in solution to these spectra can be disregarded taking into account the very weak intensity shown by the spectrum of the aqueous solution of FA (Fig. 5g). Therefore, it can be concluded that all the bands observed in the spectra of home-prepared samples and P25 TiO_2 correspond to adsorbed species. On the other hand, the spectrum of TiO_2 Merck (Fig. 5f) shows only the weak contributions of ferulic acid solution and is virtually free from bands due to adsorbed species.

The spectra of P25 TiO_2 and the three home-prepared titania samples retain essentially most of the features of FA in the 1800–900 cm^{-1} wavenumber region (Fig. 5e). Two main differences can be noticed in comparison with the spectrum of the unbounded acid. On one hand, the carbonyl stretching band of the carboxylic group at ca. 1695 cm^{-1} is completely removed in the spectra of home-prepared samples and only shows very weak intensity for P25 TiO_2. On the other hand, the spectra of the four samples show two additional overlapping broad bands centered at around 1500 and 1400 cm^{-1}, which can be respectively ascribed to the antisymmetric and symmetric OCO stretching of adsorbed

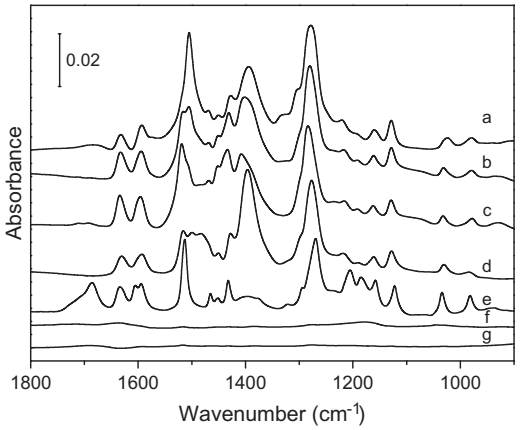

Fig. 5. ATR-FTIR spectra of titania photocatalysts HP0.5 (a), HPC3 (b), Degussa P25 (c), HP1/50 (d) and Merck anatase (f) in contact with a 0.5 mM aqueous solution of FA at room temperature in the dark for 2 h. The spectra of the 0.5 mM aqueous solution of FA (g) and FA dissolved in chloroform (e) are also shown for comparison.

ferulate. These results indicate that adsorption of FA on P25 TiO_2 and the three home-prepared titania samples takes place via carboxylate formation, in agreement with previous reports showing that adsorption of carboxylic acids on titania proceeds very fast via titanium carboxylate formation [36–41]. In general, this kind of adsorption has been shown to occur through bridging bidentate interactions. The splitting of the carboxylate bands of ferulate species adsorbed on the series of titania samples reported in this study (ca. 100 cm^{-1}) strongly supports a bidentate binding, although the relatively small value might suggest a chelate rather than bridging-type of linkage [42]. FTIR results indicate that the charge-transfer complex formed by adsorption of ferulic acid on P25 TiO_2, HP0.5, HP1/50, and HPC3 corresponds to a bidentate titanium ferulate. Adsorbed ferulate species were not detected on Merck titania, in

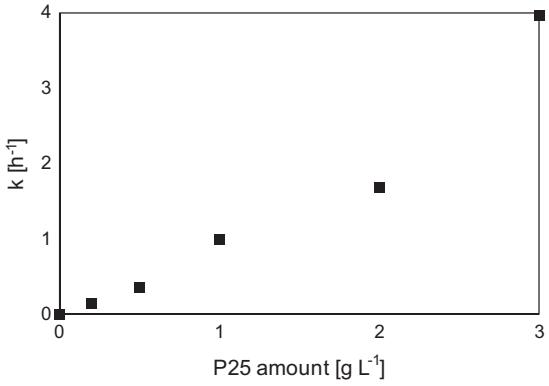

Fig. 6. First-order rate constant versus P25 TiO_2 amount.

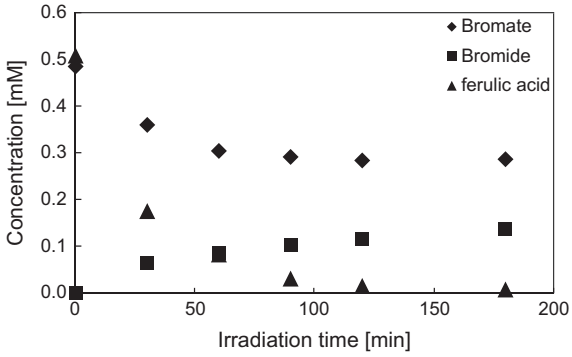

Fig. 8. FA oxidation in the absence of O_2 and in the presence of $KBrO_3$.

agreement with UV–Vis data, which showed the lack of charge-transfer complex formation on that sample.

Photocatalytic reactions are generally carried out by using a limited amount of catalyst, since an excess can produce a screening effect of particles in the nearby of the irradiation source with respect to the backward particles that remain inactive. For runs carried out by using increasing amounts of P25 TiO_2, the rate of FA degradation well fitted first-order kinetics:

$$-\frac{dC_L}{dt} = kC_L \tag{2}$$

where C_L is the FA concentration in the liquid phase, t the irradiation time, and k is the first-order rate constant. By applying a least-squares best-fitting procedure to the $C_L - t$ data, the values of k have been determined; they are reported in Fig. 6 as a function of the catalyst amount. It may be noted that the values of k linearly increase with the catalyst amount up to significant levels. This behavior is in agreement with the occurrence of a complete irradiation of all the catalyst particles inside the reactor. In the presence of the highest amount of suspended catalyst ($3\ g\ L^{-1}$) indeed, the irradiance measured outside the reactor was equal to 50% of the emitted one. As reported by Camera-Roda et al. [43], the reaction rate increases linearly with the amount of the photocatalyst regardless of the intensity of the irradiation provided that the value of the optical thickness of suspension is smaller than 1, as it is the case of the used experimental conditions.

Irradiating by visible light ($\lambda \geqslant 400$ nm), a *cis*- and *trans*-ferulic acids mixture (40:60 M ratio), prepared by a 1 h-lasting homogeneous UV photoisomerization of *trans*-ferulic acid [29], allowed to observe that the two isomers exhibit a degradation kinetics of first order expressed by Eq. (2). The values of k were $4.3 \times 10^{-3}\ mM\ min^{-1}$ and $5.2 \times 10^{-3}\ mM\ min^{-1}$ for *cis*- and *trans*-ferulic acids, respectively, indicating that both isomers show the same reactivity. Furthermore, values of conversion and selectivity to vanillin were comparable, starting just from *trans*-ferulic acid or from a *cis–trans* mixture. Indeed, after 1-h visible irradiation in both cases, the conversion was about 60% and the selectivity to vanillin was about 2% for a standard reaction using P25 TiO_2.

The optical electron transfer from FA to the conduction band of TiO_2, known in literature for molecules like cathecol, enediols, and chlorophenols [44], could occur through the following reaction steps:

$$TiO_2 + FA \rightarrow [TiO_2 - FA] \tag{3}$$

$$[TiO_2 - FA] \xrightarrow{h\nu} TiO_2\left(e^-_{CB}\right) - FA^{\cdot+} \tag{4}$$

$$O_2 + e^-_{CB} \rightarrow\rightarrow \cdot OH \tag{5}$$

$$FA^{\cdot+}_{(s)} + H_2O \rightarrow \cdot OH + H^+ + FA_{(s)} \tag{6}$$

$$FA^{\cdot+}_{(s)} \xrightarrow{h\nu} \xrightarrow{h\nu} \text{oxidation intermediates} \xrightarrow{h\nu} CO_2 \tag{7}$$

In order to support the reported mechanism, some experiments have been performed by oxidizing FA in the presence of a phosphate-modified P25 TiO_2. The runs showed that the FA oxidation rate decreases of ca. 50%. It is indeed well known that phosphate ions adsorb strongly thanks to electrostatic interactions between anions and catalyst surface and react with the surface hydroxyl groups, without modifying the electronic features of the catalysts [45]. As a final result, they are able either to block active sites or to compete with organic species during the photocatalytic processes, thus reducing the global rate of oxidation of target compounds.

For an initial pH in the 3.2–3.9 range, the catalyst color got yellowish in the presence of FA, whereas water remained uncolored. By increasing the initial pH by using NaOH 1 M solution, a decrease in conversion was observed down to 0% at pH = 12, due to the lack of adsorption of the anionic species on TiO_2 surface. FA is indeed characterized by the equilibriums reported in Fig. 7, and the pH strongly influences the species existing in water.

Nevertheless, Merck TiO_2 did not give rise neither to conversion nor to adsorption of FA at any initial pH values. A prominent role in the absence of activity is probably played by characteristic features of the solid surface (such as limited hydroxylation).

In order to better investigate the reaction mechanism, some runs were carried out in the virtual absence of O_2, by continuously bubbling N_2 in the suspension. As expected, the anaerobic conditions determined the total inhibition of the FA degradation. In anaerobic conditions but in the presence of bromate ions, high FA conversions were observed. Bromate ions played indeed the role of oxidant agent, reducing to bromide ions, by accepting electrons from the

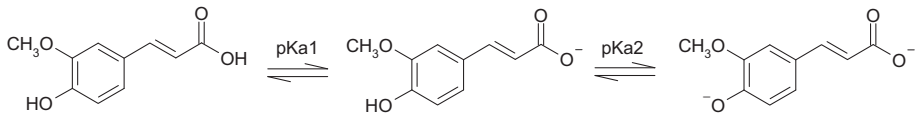

Fig. 7. Ferulic acid acid–base equilibrium.

excited charge-transfer complex formed between FA and TiO_2. Accordingly, Fig. 8 shows that once FA has been completely converted, bromate ions concentration did not change, thus demonstrating that the reactivity is due to the complex activity.

4. Conclusions

FA has been oxidized through the formation of a charge-transfer complex with some specific TiO_2 samples under visible irradiation. The most abundant detected products were CO_2 and vanillin. Interaction between FA and TiO_2 has been deeply investigated in order to hypothesize adsorption and reaction mechanisms. The former one was modelled by means of Langmuir adsorption isotherms and detailed by means of ATR FT-IR, allowing to understand that FA adsorption on TiO_2 surface occurs via carboxylate formation, and that the absence of adsorption in the presence of TiO_2 Merck, SiO_2, and Al_2O_3 is the reason of the lack of reactivity. Accordingly to the reported evidence, reactivity was found to follow the same trend of adsorbed FA amounts on TiO_2 samples. Finally, the more hydroxylated was TiO_2 surface (found by means of TGA measurements) the higher the reactivity.

References

[1] M. Schiavello (Ed.), Photocatalysis and Environment Trends and Applications, Kluwer Academic Pu., Dordrecht, 1988.
[2] D.F. Ollis, H. El-Ekabi (Eds.), Photocatalytic Purification and Treatment of Water and Air, Elsevier Science Publ., New York, 1993.
[3] M. Schiavello (Ed.), Heterogeneous Photocatalysis, Wiley Series in Photoscience and Photoengineering, vol. 3, J. Wiley & Sons., Chichester, 1997.
[4] M. Schiavello (Ed.), Photoelectrochemistry, Photocatalysis, and Photoreactors Fundamentals and Developments, Reidel, Dordrecht, 1985.
[5] E. Pelizzetti, N. Serpone (Eds.), Homogeneous and Heterogeneous Photocatalysis, Reidel, Dordrecht, 1986.
[6] N. Serpone, E. Pelizzetti (Eds.), Photocatalysis, Fundamentals and Applications, J. Wiley & Sons, Chichester, 1989.
[7] K. Takahama, N. Nakagawa, K. Kishimoto, JP 09192496 A2, 1997.
[8] J. Choi, H. Park, M.R. Hoffmann, J. Phys. Chem. C 114 (2010) 783.
[9] P.V. Kamat, Chem. Rev. 93 (1993) 267.
[10] B. O'Regan, M. Grätzel, Nature 353 (1991) 737.
[11] S. Sakthivel, H. Kisch, Angew. Chem. Int. Ed. 42 (2003) 4908.
[12] W. Zhao, W.H. Ma, C.C. Chen, J.C. Zhao, Z.G. Shuai, J. Am. Chem. Soc. 126 (2004) 4782.
[13] Q. Wang, C.C. Chen, W.H. Ma, H.Y. Zhu, J.C. Zhao, Chem. Eur. J. 15 (2009) 4765.
[14] C.C. Chen, W.H. Ma, J.C. Zhao, Curr. Org. Chem. 14 (2010) 630.
[15] S.-I. Naya, A. Inoue, H. Tada, J. Am. Chem. Soc. 132 (2010) 6292.
[16] D. Pei, J. Luan, Int. J. Photoenergy ID 262831, 2012, 13p.
[17] N.M. Dimitrijevic, E. Rozhkova, T. Rajh, J. Am. Chem. Soc. 131 (2009) 2893.
[18] Y. Park, N.J. Singh, K.S. Kim, T. Tachikawa, T. Majima, W. Choi, Chem. Eur. J. 15 (2009) 10843.
[19] X. Li, C. Chen, J. Zhao, Langmuir 17 (2001) 4118.
[20] Y. Cho, H. Kyung, W. Choi, Appl. Catal. B: Environ. 52 (2004) 23.
[21] F. Parrino, A. Ramakrishnan, H. Kisch, Angew. Chem. In. Ed. 47 (2008) 7107.
[22] G. Kim, W. Choi, Appl. Catal. B: Environ. 100 (2010) 77.
[23] A.G. Agrios, K.A. Gray, E. Weitz, Langmuir 19 (2003) 1402.
[24] A.G. Agrios, K.A. Gray, E. Weitz, Langmuir 20 (2004) 5911.
[25] S. Kim, W. Choi, J. Phys. Chem. B 109 (2005) 5143.
[26] S. Higashimoto, N. Kitao, N. Yoshida, T. Sakura, M. Azuma, H. Ohue, Y. Sakata, J. Catal. 266 (2009) 279.
[27] B. Abramović, D. Šojić, V. Anderluh, Acta Chim. Slov. 54 (2007) 558.
[28] A.M. Amat, A. Arques, F. Galindo, M.A. Miranda, L. Santos-Juanes, R.F. Vervher, R. Vicente, Appl. Catal. B: Environ. 73 (2007) 220.
[29] V. Augugliaro, G. Camera-Roda, V. Loddo, G. Palmisano, L. Palmisano, F. Parrino, M.A. Puma, Appl. Catal. B: Environ. 111–112 (2012) 555.
[30] V. Augugliaro, T. Caronna, V. Loddo, G. Marcì, G. Palmisano, L. Palmisano, S. Yurdakal, Chem. Eur. J. 14 (2008) 366.
[31] S. Yurdakal, G. Palmisano, V. Loddo, O. Alagöz, V. Augugliaro, L. Palmisano, Green Chem. 11 (2009) 510.
[32] G. Palmisano, V. Loddo, S. Yurdakal, V. Augugliaro, L. Palmisano, Adv. Synth. Catal. 349 (2007) 964.
[33] G. Kortüm, Reflectance Spectroscopy: Principles, Methods, Applications, Springer-Verlag, New York, 1969.
[34] R. Mueller, H.K. Kammler, K. Wegner, S.E. Pratsinis, Langmuir 19 (2003) 160.
[35] G. Palmisano, V. Loddo, V. Augugliaro, L. Palmisano, S. Yurdakal, AIChE J. 53 (2007) 961.
[36] S. Tunesi, M. Anderson, J. Phys. Chem. 95 (1991) 3399.
[37] K.D. Dobson, A.J. McQuillan, Spectrochim. Acta A 55 (1999) 1395.
[38] K.D. Dobson, A.J. McQuillan, Spectrochim. Acta A 56 (1999) 557.
[39] D. Robert, S. Parra, C. Pulgarin, A. Krzton, J.V. Weber, Appl. Surf. Sci. 167 (2000) 51.
[40] F.P. Rotzinger, J.M. Kesselman-Truttmann, S.J. Hug, V. Shklover, M. Grätzel, J. Phys. Chem. B 108 (2004) 5004.
[41] P.C. Angelomé, G.J. de A.A. Soler-Illia, Chem. Mater. 17 (2005) 322.
[42] K. Nakamoto, Infrared and Raman Spectra of Inorganic and Coordination Compounds, fifth ed., Wiley-Interscience, New York, 1997.
[43] G. Camera-Roda, F. Santarelli, M. Panico, Photochem. Photobiol. Sci. 8 (2009) 712.
[44] S.C. Li, L.N. Chu, X.Q. Gong, U. Diebold, Science 328 (2010) 882.
[45] M. Abdullah, G.K.-C. Low, R.W. Matthews, J. Phys. Chem. 94 (1990) 6820.